

Electronic Supplementary Information

Ternary Memory Module Using Low-Voltage Control over Optical Properties of Metal-Polypyridyl Monolayers†

† A Tribute to Late Dr. Tarkeshwar Gupta

**Anup Kumar^a, Megha Chhatwal^a, Prakash C. Mondal^a, Vikram Singh^a, Alok Kumar
Singh^a, Domenico A. Cristaldi^b, Rinkoo D. Gupta^{c*} and Antonino Gulino^{b*}**

Experimental Section:

Materials and methods: Most of the chemicals *viz.* 2-acetyl pyridine, *p*-tolualdehyde, *N*-bromosuccinimide, $\text{RuCl}_3 \cdot x\text{H}_2\text{O}$, and $(\text{NH}_4)_2(\text{OsCl}_6)$ were purchased from Sigma Aldrich and used without further purification. $\text{NaClO}_4 \cdot x\text{H}_2\text{O}$ and hexamethyltetraamine were bought from Alfa Aesar. Potassium tert-butoxide and 1, 10 phenanthroline were purchased from Spectrochem. Pvt. Ltd. Methanol and ethanol were purchased from Merck and were distilled using reported method^{S1} before use. Dry *n*-pentane, toluene, 30% aq. ammonia, and H_2O_2 , (all AR grade) were purchased from S. D. Fine Chemicals (India). The acetonitrile used was always distilled using CaH_2 before each experiment. Double distilled water was used for washing and rinsing purpose. Deuterated solvents were purchased from Aldrich and stored under freezer. Single-crystal silicon [100] substrates were imported from Beschichtungen (Silz, Germany). Indium-tin-oxide coated glass was purchased from Scientific Technologies (India). Hydrothermal bombs (25mL & 50mL) were purchased from Prakash Scientific Works (India) for monolayer fabrication.

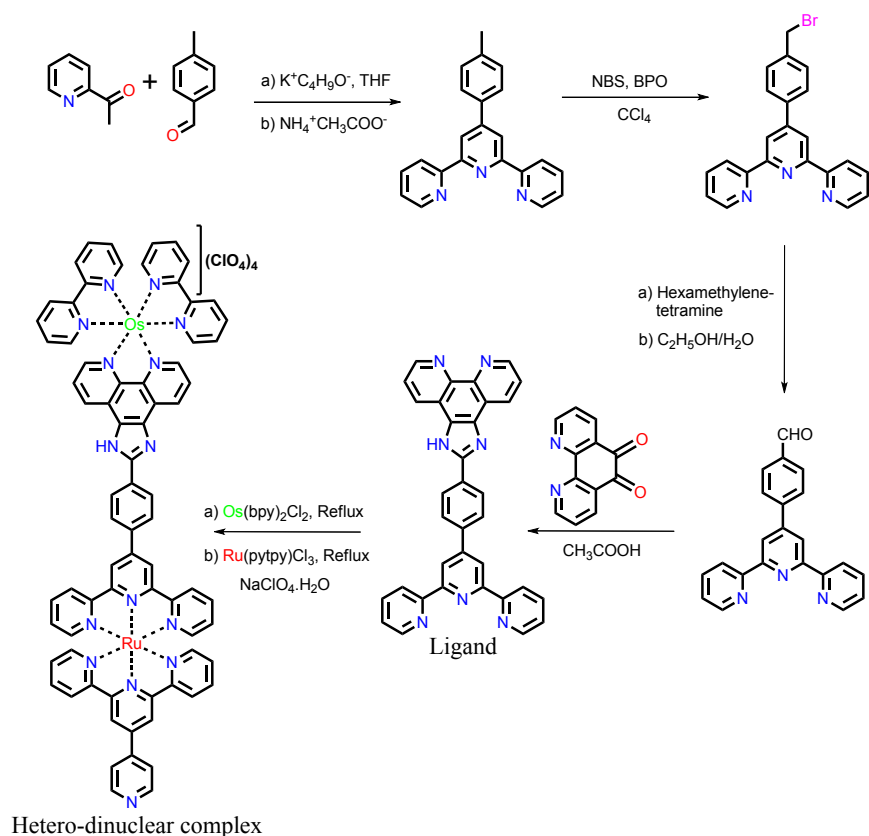
4'-(*p*-Tolyl)-2,2':6'2'' terpyridine^{S2}, 4'-(Phenyl-*p*-bromomethyl)-2,2': 6',2''-terpyridine^{S3}, 4'-(Phenylcarbonyl)-2,2':6',2''-terpyridine^{S4}, 1,10-phenanthroline-5,6-dione^{S5}, 2-(4-([2,2':6',2''-terpyridin]-4'-yl)phenyl)-1H-imidazo[4,5-f][1,10]phenanthroline^{S6}, $\text{Os}(\text{bpy})_2\text{Cl}_2$ ^{S7} and $\text{Ru}(\text{pytpy})\text{Cl}_3$ ^{S8} were synthesised using reported methods and characterised by ¹H-NMR, mass, infrared, and UV-vis spectroscopy.

UV-vis spectroscopy was carried out using JASCO UV-vis-NIR spectrophotometer (V670). Mass spectra were recorded on ESI-MS mass spectrometer (Dept. of Chemistry, University of Delhi, India). CHI-660D electrochemical workstation having conventional three electrode configuration consisting of glassy carbon as working electrode, platinum wire as counter electrode and aqueous Ag/AgCl as reference electrode, was used to carry out electrochemical measurements. The spectro-electrochemical switching experiment was done with Basispectro-electrochemical kit with porous glassy carbon electrode as working, Ag/AgCl as

reference and spring-type Pt wire electrode as counter electrode. All $^1\text{H-NMR}$ spectra were recorded on Jeol JNMECX 400P spectrometer. All chemical shifts (δ) are reported in ppm, and coupling constants (J) are in Hz relative to tetramethylsilane. All measurements were carried out at ambient temperature unless otherwise stated.

Angle resolved X-ray photoelectron spectra (AR-XPS) were measured at different photoelectron take-off angles (5° , 15° , 45° and 80°) relative to the surface plane with a PHI 5600 Multi Technique System which gives good control of the electron take-off angle (base pressure of the main chamber 2×10^{-10} Torr)^{S9}. Spectra were excited with monochromatized Al-K α radiation. XPS peak intensities were obtained after Shirley background removal.^{S9c} Spectra calibration was achieved by fixing the main C 1s peak at 285.0 eV.^{S9} Experimental uncertainties in binding energies lie within ± 0.3 eV. Fitting of the N 1s spectra was carried out by fitting the spectral profile with symmetrical Gaussian peaks after subtraction of the background. This process involves data refinement, based on the method of the least squares fitting, carried out until there was the highest possible correlation between the experimental spectrum and the theoretical profile. The R-factor (residual or agreement factor), $R = [\Sigma(\text{Fo} - \text{Fc})^2 / \Sigma (\text{Fo})^2]^{1/2}$, after minimization of the function $\Sigma(\text{Fo} - \text{Fc})^2$ converged to R values ≤ 0.021 .^{S10}

Atomic force microscopy (AFM) measurements were performed with a Solver P47 NTD-MDT instrument in semi-contact mode (resonance frequency 150 Hz). The noise level before and after each measurement was confined within ± 0.01 nm.



Scheme 1: Proposed synthetic route for hetero-dinuclear complex.

Synthesis of Os-Mononuclear precursor: To a solution of $\text{Os}(\text{bpy})_2\text{Cl}_2$ (50 mg, 87 μmol) in absolute ethanol (20 ml), ligand (45 mg, 87 μmol) was added and the resulting solution was refluxed for 72 h. The contents were then filtered and reduced to 5ml before precipitating by addition of an excess of $\text{NaClO}_4 \cdot \text{H}_2\text{O}$. The complex was filtered and washed with ample amount of water followed by diethyl ether and purified by column chromatography using alumina (neutral, activity G-III) and acetonitrile–water (70:30 v/v) as eluent. The second dark green fraction was collected, dried under vacuum and recrystallised by slow vapour-diffusion of diethyl ether into acetonitrile solution of the complex. Yield: 55mg (52%). $^1\text{H-NMR}$ (400 MHz, $\text{DMSO-}d_6$, δ/ppm) 14.56 (s, 1H, NH imidazole), 8.92 (d, 2H, $J = 8.0$ Hz), 8.89-8.77 (m, 10H), 8.71 (d, 2H, $J = 7.85$ Hz), 8.55 (d, 2H, $J = 8.49$ Hz), 8.30 (d, 2H, $J = 8.43$ Hz), 8.09-7.96 (m, 6H), 7.94-7.81 (m, 2H), 7.76 (d, 2H, $J = 5.27$ Hz), 7.59-7.43 (m, 6H), 7.29-7.21 (m, 2H). ESI-MS: (m/z): 343.8271 (22%) $[\text{M-C}_{22}\text{H}_{15}\text{N}_5]^2+$, 515.8608 (100%) $[\text{M-}$

$2\text{ClO}_4]^{2+}$, 1027.8329 (5%) $[\text{M}-2\text{ClO}_4]$, 1129.6129 (10%) $[\text{M}-\text{ClO}_4]$: UV-vis ($\lambda_{\text{max}}/\text{nm}$, $\epsilon/M^{-1}\text{cm}^{-1}$): 290 (1, 16, 441), 328 (51,844), 434 (18,158), 484 (19,662), 635 (4385). CV (10^{-3}M , CH_3CN): $E^1_{1/2} = 0.9265$ ($\text{Os}^{2+}/\text{Os}^{3+}$), $\Delta E = 70\text{mV}$ at 300mVs^{-1} .

Synthesis of hetero-dinuclear complex: To a solution of Osmium mononuclear precursor (50 mg, 40 μmol) in 30 ml of degassed ethylene glycol, $\text{Ru}(\text{pytpy})\text{Cl}_3$ (20 mg, 40 μmol) was added with a few drops of *N*-ethylmorpholine and the resulting solution was refluxed for 12 h.^{S10} After concentrating the solution under vacuum, the complex was precipitated by addition of an excess $\text{NaClO}_4\cdot\text{H}_2\text{O}$. After filtration, the product was washed with ample amount of water and diethyl ether. Finally, complex was purified by column chromatography (neutral alumina, acetonitrile: water, 70:30) and recrystallised with diffusion of diethyl ether over acetonitrile solution of complex. Yield = 31mg (43%). $^1\text{H-NMR}$ (400 MHz, $\text{DMSO}-d_6$, δ/ppm) 9.07 (d, 4H, $J = 6.76$ Hz), 8.97 (s, 1H), 8.91-8.87 (m, 3H), 8.67-8.58 (m, 4H), 8.47-8.38 (dd, 6H, $J = 7.32$ Hz, $J = 7.56$ Hz), 8.38-8.32 (m, 2H), 8.07 (dd, 2H, $J = 1.2$ Hz, $J = 4.3$ Hz), 7.94-7.62 (m, 15H), 7.60 (dd, 2H, $J = 5.99$ Hz, $J = 5.90$ Hz), 7.46 (d, 2H, $J = 6.3$ Hz), 7.41 (dd, 1H, $J = 1.0$ Hz, $J = 5.0$ Hz), 7.34 (dd, 2H, $J = 1.0$ Hz, $J = 5.0$ Hz), 7.27 (td, 1H, $J = 6.1$ Hz, $J = 7.6$ Hz, $J = 1.3$ Hz), 7.17 (m, 4H), 7.05 (t, 2H, $J = 6.1$ Hz, $J = 6.7$ Hz, $J = 6.0$ Hz). ESI-MS: (m/z): 359.13 $\{[\text{M}-[\text{ClO}_4]_4\}^{4+}$: UV-vis ($\lambda_{\text{max}}/\text{nm}$, $\epsilon/M^{-1}\text{cm}^{-1}$): 288 (98,154), 435 (24,764), 494(44,863), 643 (4038). CV (10^{-3}M , CH_3CN): $E^1_{1/2} = 0.91$ ($\text{Os}^{2+}/\text{Os}^{3+}$), $E^2_{1/2} = 1.37$ ($\text{Ru}^{2+}/\text{Ru}^{3+}$), $\Delta E^1 = 87$ mV, $\Delta E^2 = 73$ mV at 300mVs^{-1} .

Monolayer Formation. Si(100) and ITO substrates were cleaned by sonication in hexane, followed by acetone, then ethanol and dried under an N_2 stream. Subsequently, they were heated in an oven for 2 hours at 120°C . Freshly cleaned ITO coated glass and silicon substrate were placed into a Teflon holder in a 100 ml beaker which was filled with ~ 80 ml dry *n*-pentane in glove box (O_2 level < 0.5 ppm). An excess of 3-iodo-*n*-propyl-1-trimethoxysilane (coupling reagent, 100 μl) was added to this dry pentane solution and the

solution was kept undisturbed for 30 min. The coupling reagent functionalized substrates were then sonicated with *n*-pentane, dichloromethane, isopropanol for 6 min each and dried at 120°C for further 30 min. Finally, the substrates were maintained at room temperature and loaded into the Teflon-coated hydrothermal bomb in dry acetonitrile/toluene (8:2 v/v) solution (0.5 mM) of hetero-dinuclear complex and heated for 60 h at 80°C with the exclusion of light. The functionalized substrates were then sonicated with acetonitrile, dichloromethane and isopropanol for 6 min each to remove any physisorbed material. The monolayers were wiped with a task wipe, then dried under a stream of N₂ and stored in the dark. The monolayer films were analysed with UV/vis spectroscopy, cyclic voltammetry, XPS and AFM.

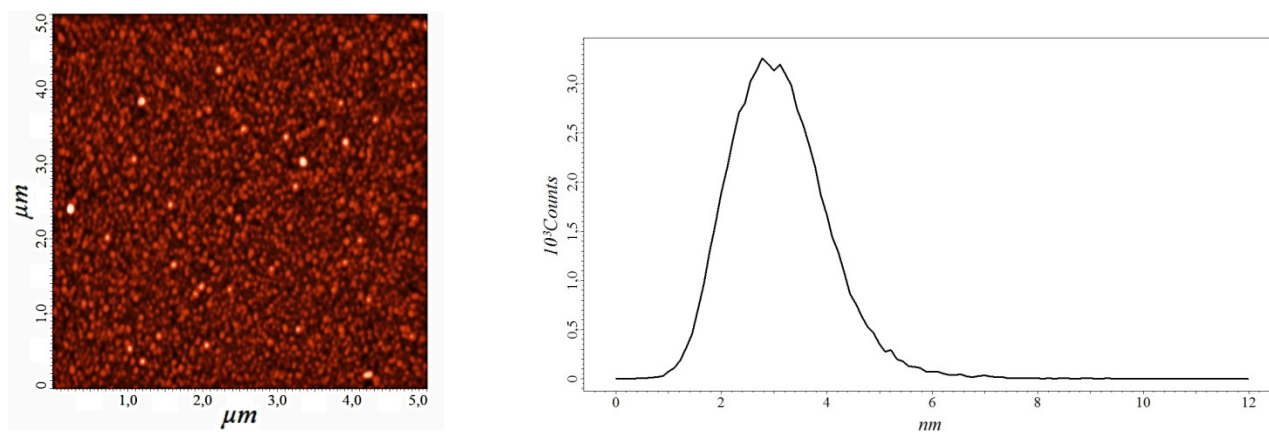


Figure S1: AFM image (left) and height profile (right) of a representative **1-Si(100)** monolayer.

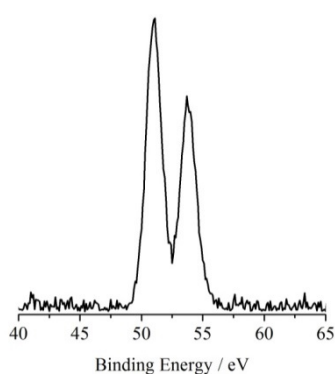


Figure S2: Monochromatized Al-K α excited XPS at 45° photoelectron take-off angle for a **1-Si(100)** monolayer in the Os 4f binding energy region.

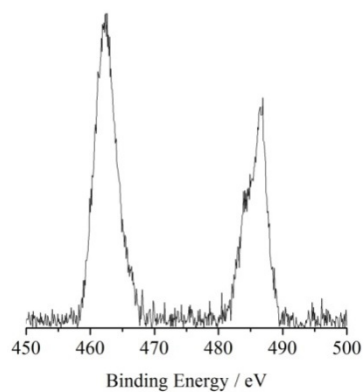


Figure S3: Monochromatized Al-K α excited XPS at 45° photoelectron take-off angle for a **1-Si(100)** monolayer in the Ru 3p binding energy region.

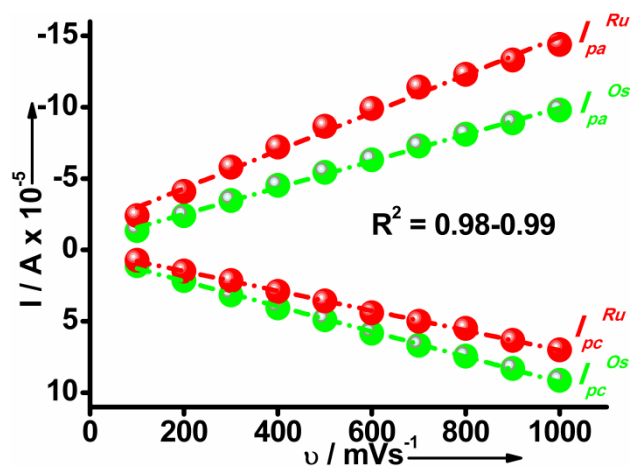


Figure S4: Plot showing linear fit of peaks current as a function of scan rates.

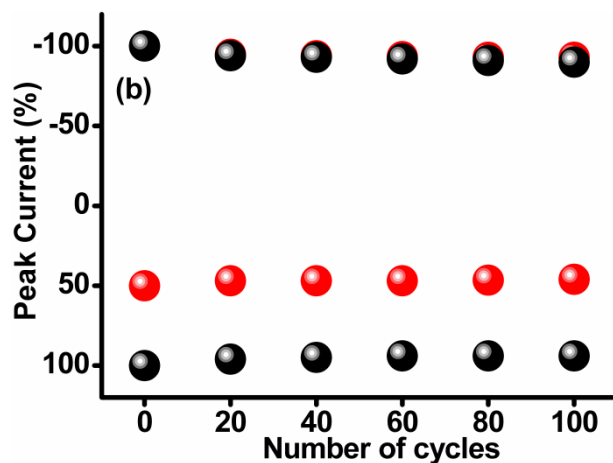


Figure S5: Read-write cycles of 1-ITO monolayer for osmium metal centre (black balls) and ruthenium metal centre (red balls) for 100 cycles.

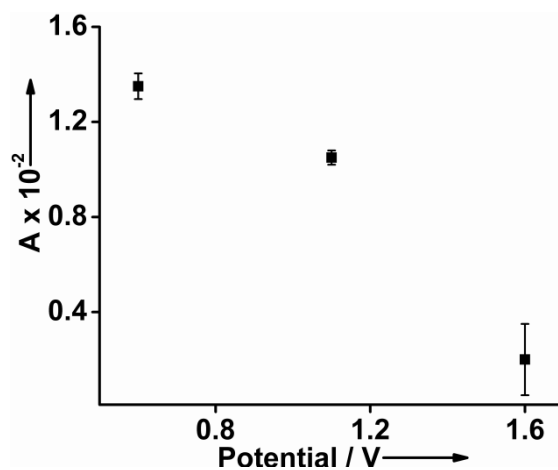


Figure S6: Triple-step potential based-switching at ¹MLCT for 1-ITO monolayer using same set-up for three times.

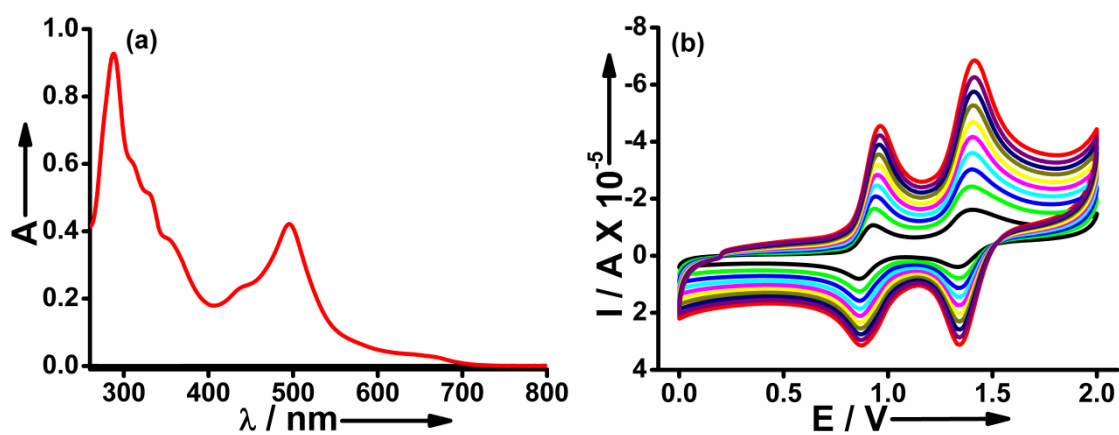


Figure S7: UV-vis spectrum of hetero-dinuclear complex ($0.96 \times 10^{-5}\text{M}$, CH_3CN) at ambient temperature (a), Cyclic voltammetric responses of hetero-dinuclear complex ($0.98 \times 10^{-3}\text{M}$, 0.1M TBAP, CH_3CN) at different scan rates ranging from $100\text{-}1000\text{ mVs}^{-1}$.

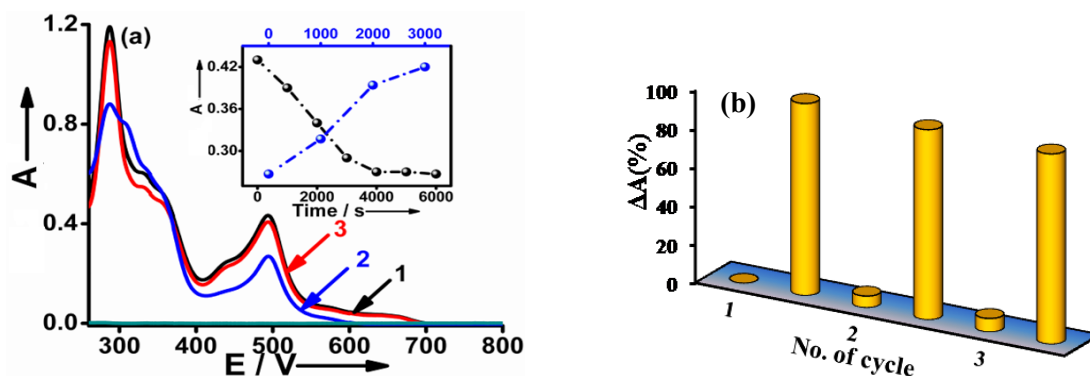


Figure S8: Absorbance intensity changes on electrochemical tuning of osmium centre of hetero-dinuclear complex ($1.1 \times 10^{-5}\text{M}$, 20 mM TBAP in acetonitrile) in its initial spectrum (1) on applying 1.1V (oxidation potential) (2), on applying 0.6V (reduction potential) (3). Inset: representative plot for showing gradual absorbance change on applying oxidation potential 1.1V (black balls) and reduction potential 0.6V (blue balls) (a) and bar chart for showing $\Delta A(\%)$ at 493nm vs. number of alternative redox cycles (b).

Electrochromic test: Segregative tuning of optical identity of osmium. The acetonitrile solution of hetero-dinuclear complex ($1.1 \times 10^{-5}\text{M}$, 20 mM TBAP, 50 ml) was poured into the spectro-electrochemical setup. Subsequently, the solution was purged with N_2 gas with mild stirring for 15 min . Finally, the oxidation potential of 1.1V which is suitable for oxidation of only osmium centre was applied. Simultaneously, the UV-vis spectrum was also taken with the interval of 1000s till no further changes were observed in spectrum/full-oxidation of Os-centre (6000s). Now, the applied potential was shifted to reduction potential of osmium centre which is 0.6 V in above system and UV-vis spectrum was taken after every 1000s till the reappearing of initial data. Above mentioned methodology was executed for 3 cycles to judge the reversibility of system.

Electrochromic test: Selective and interference-free address of optical property of osmium and ruthenium metal centre. The acetonitrile solution of **1** ($1.1 \times 10^{-5}\text{M}$, 20 mM TBAP, 50 ml) was poured into the spectro-electrochemical setup. Subsequently, the solution was purged with N_2 gas with mild stirring for 15 min . Finally, the solution was subjected to oxidation potential of osmium metal centre (1.1V) for 6000s . UV-vis spectrum was also

taken with the interval of 1000s till no further changes were observed in spectrum/full-oxidation of Os-centre (6000s). Now, the applied potential was shifted to oxidation potential of ruthenium centre 0.6 V and UV-vis spectrum was taken after every 1000s till full oxidation of ruthenium metal centre. Further, the potential was shifted to reduction mode of ruthenium by applying a potential of 1.0V for 3000s and then, potential of 0.6V for reduction of osmium metal centre. The above mentioned methodology was executed for 3 cycles to judge the reversibility of system.

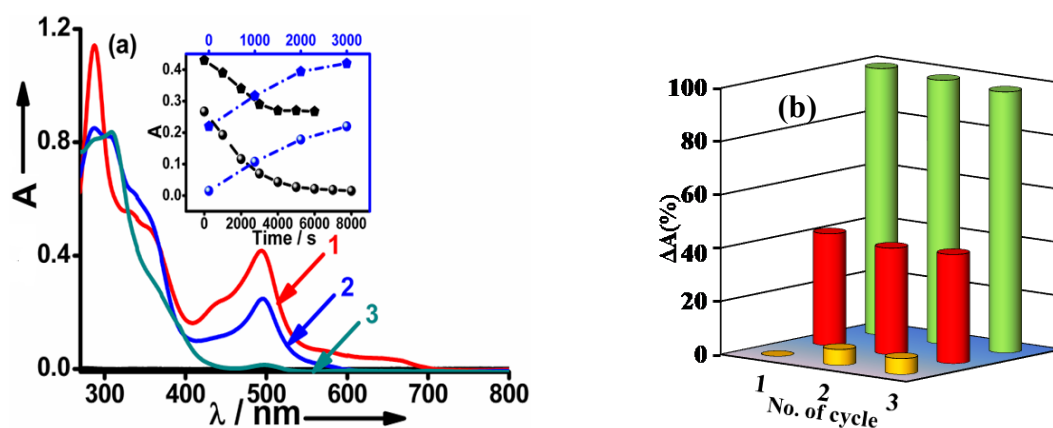


Figure S9: Absorbance intensity changes on stepwise electrochemical tuning of osmium and ruthenium centre of hetero-dinuclear complex ($1.1 \times 10^{-5}M$, 20 mM TBAP in acetonitrile) in its initial spectrum (1), on applying 1.1V (oxidation potential for osmium) (2), on applying 1.6V (oxidation potential for ruthenium) (3). Inset: representative plot for showing gradual absorbance change on applying oxidation potential 1.6 and 1.1V (black balls and pentagon) and reduction potential 1.0 and 0.6 V (blue balls and pentagon) (a) and bar chart for showing stepwise $\Delta A(\%)$ at 493nm vs. number of 3 alternative redox cycles (b).

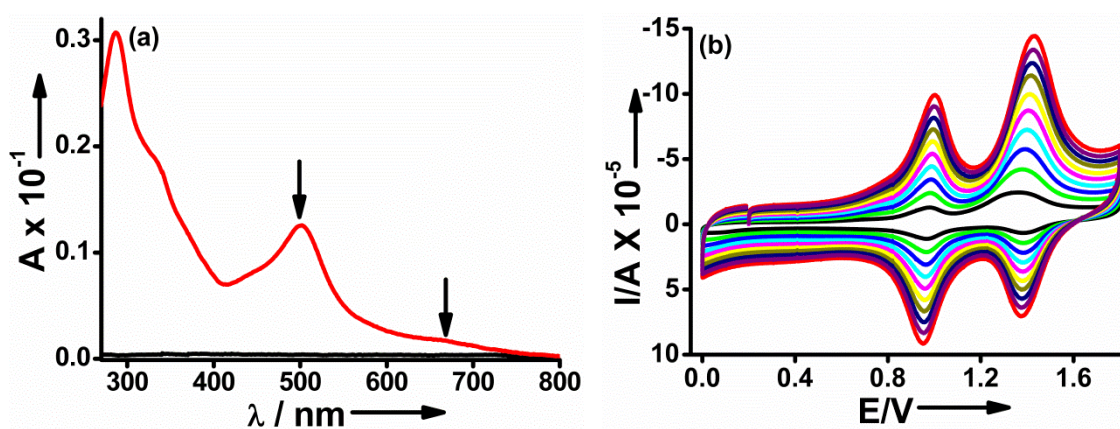


Figure S10: UV-vis spectrum of **1-ITO** monolayer (0.8×3 cm, CH_3CN) at ambient temperature (a), Cyclic voltammetric responses of **1-ITO** monolayer (0.8×3 cm, 20mM TBAP, CH_3CN) at different scan rates ranging from 100-1000 mVs^{-1} .

Details of switching experiment on monolayer: The **1-ITO** monolayer was kept in quartz cuvette which was filled with TBAP solution (20mM, CH_3CN). The monolayer was set-up as working electrode while aqueous Ag/AgCl and platinum wire was used as reference and counter electrode respectively. The background correction was done with a blank ITO slide in dipped in TBAP solution in reference cuvette. After fixing the electrodes, the potential range (0.6-1.1V) for oxidation and reduction of osmium metal centre was applied and corresponding absorbance changes were recorded using UV-vis instrument. Then, a wider potential range (0.6-1.6V) was applied for redox cycle of ruthenium and osmium both. Finally, the potential step of 0.6-1.1-1.6V was applied for segregative knocking of metal centre with respective absorbance changes. The switching experiments were repeated for 100 cycles.

Thermal and temporal stability: The **1**-based monolayer was subjected to thermal stress to judge the effect of temperature. The samples were placed inside a sealed glass pressure tube with open lid. The thermal stability was monitored by ex-situ UV-vis measurements at $200 \pm 5^\circ\text{C}$ for varying time intervals (*i.e.*, 0, 5, 10, 15, 20, 25, 30, 35, 40, 45 and 50h). The temporal stability was monitored by keeping the samples for $>1\text{h}$ at various temperatures (*i.e.*, 25, 50, 75, 100, 125, 150, 175, 200, 225 and 250°C). Before each temperature increase, the samples were allowed to attain room temperature, rinsed with CH_3CN , gently wiped with task paper and analyzed by UV-Vis spectrophotometry.

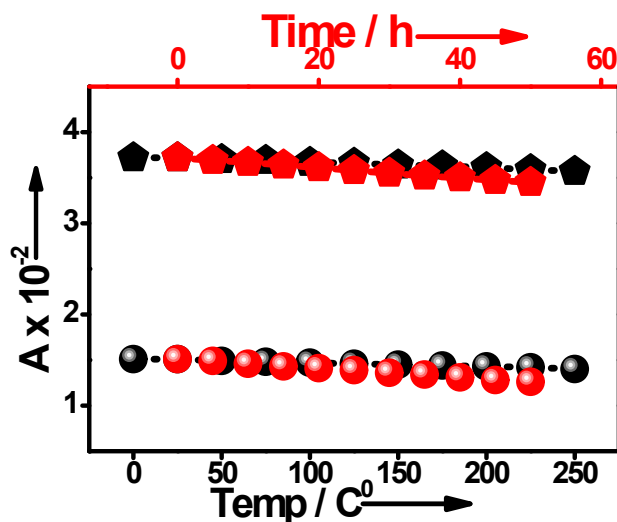


Figure S11: UV-Vis monitoring of the 1-ITO monolayer on ITO-coated glass at various temperatures and time intervals. Red and black data points represent the absorbance at ¹MLCT and LC band after temporal and thermal stability respectively.

References:-

- S1. D. D. Perrin and W. L. F. Armarego, *Purification of Laboratory Chemicals*, 3. Aufl., Oxford. Pergamon Press, 1988.
- S2. F. Tessore, D. Roberto, R. Ugo and M. Pizzotti, *Inorg. Chem.*, 2005, **44**, 8967-8978.
- S3. Z-J. Hu, J-X. Yang, Y-P. Tian, H-P. Zhou, X-T. Tao, G-B. Xu, W-T Yu, X-Q Yu, M-H. Jiang, *J. Biomol. Struct.*, 2007, **839**, 50-57.
- S4. J-P. Collin, A. Harriman, V. Heitz, F. Odobel and J-P. Sauvage, *J. Am. Chem. Soc.*, 1994, **116**, 5679-5690.
- S5. W. Guo, B. J. Engelman, T. L. Haywood, N. B. Blok, D. S. Beaudoin, S. O. Obare, *Talanta*, 2011, **87**, 276-283.
- S6. O. Hamelin, P. Guillo, F. Loiseau, M-F. Boissonnet, and S. Ménage, *Inorg. Chem.*, 2011, **50**, 7952-7954.
- S7. Y. Nakabayashi, K. Nakamura, M. Kawachi, T. Motoyama and O. Yamauchi, *J. Biol. Inorg. Chem.*, 2003, **8**, 45-52.
- S8. E. C. Constable, P. Harverson, C. E. Housecroft, E. Nordlander, J Olsson, *Polyhedron*, 2006, **25**, 437-458.
- S9. A. Gulino, *Anal. Bioanal. Chem.* 2013, **405**, 1479-1495; (b) D. Briggs, J. T. Grant, *Surface Analysis by Auger and X-Ray Photoelectron Spectroscopy*, IMP Publications, Chichester, UK, 2003; (c) A. Gulino, R. G. Egdell, I. Fragalà, *J. Mater. Chem.*, 1996, **11**, 1805-1809; (d) A. Gulino, G. Fiorito, I. Fragalà, *J. Mater. Chem.* 2003, **13**, 861-865.
- S10. M. Zharnikov, *J. Electron. Spectrosc.* 2010, **380**, 178-179.
- S10. (a) D. Saha, S. Das, D. Maity, S. Dutta, S. Baitalik, *Inorg. Chem.* 2011, **50**, 46-61. (b) R. Padilla, R. R. Ruminski, V. A. M. McGinley, P. B. Williams, *Polyhedron*, 2012, **33**, 158-165. (c) C. Chiorboli, M. A. J. Rodgers, F. Scandola, *J. Am. Chem. Soc.* 2003, **125**, 483-491. (d) C. Kleverlaan, M. Alebbi, R. Argazzi, C. A. Bignozzi, *Inorg. Chem.* 2000, **39**, 1342-1343.

(e) M. M. Richterf, K. J. Brewer, *Inorg. Chem.* 1993, **32**, 5762-5768. (f) L. De Cola, F. Barigelletti, V. Balzani, R. Hage, J. G. Haasnoot, J. Reedijk, *Chem. Phys. Lett.* 1991, **178**, 491-496.